AD-A079 790 NAVAL SURFACE WEAPONS CENTER DAHLGREN LAB VA F/G 8/5
SURFACE HARMONIC EXPANSIONS AND MEAN GRAVITY ANOMALIES.(U)
SEP 79 J V SHEBALIN
UNCLASSIFIED NSWC/TR-79-154 NL

END
DATE FILMED
2 80
DTIC

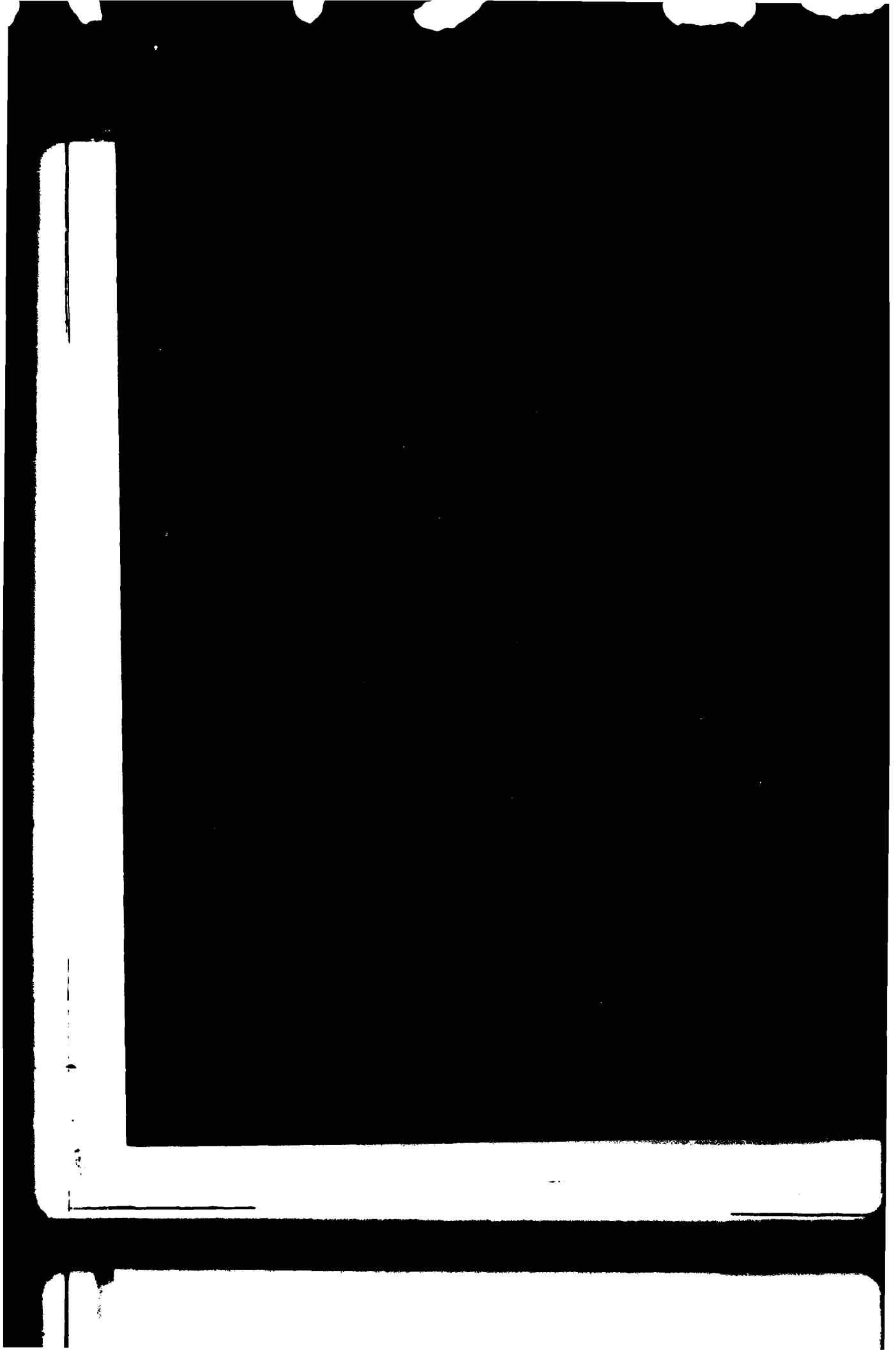

FOREWORD

This work was done in the Fire Control Presetting Analysis Branch of the FBM Geoballistics Division, Strategic Systems Department, Naval Surface Weapons Center (NSWC). It is a product of the ongoing effort at NSWC to develop and implement efficient methods for calculating the effects of anomalous gravity on missile trajectories. The work was authorized under Strategic Systems Project Office Task Assignment 37430.

This technical report was reviewed and approved by D. L. Owen, J. R. Fallin, and C. W. Duke, Jr., of the FBM Geoballistics Division.

Released by

R. T. RYLAND, Jr., Head
Strategic Systems Department

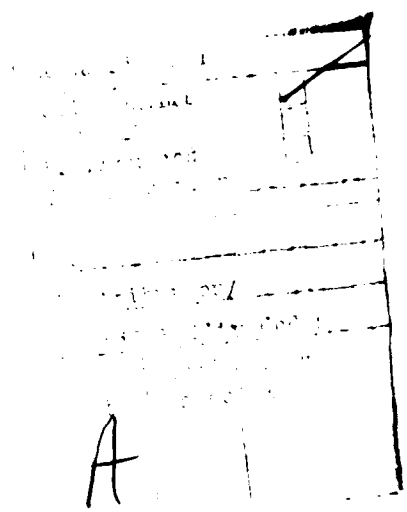

CONTENTS

INTRODUCTION

An important source of information concerning the surface harmonic expansion coefficients of the geopotential is to be found in the set of $5° \times 5°$ global mean gravity anomalies. These mean anomalies, however, because of their finite number, have an intrinsic limit on the amount of information they contain; this limit can be conveniently identified with the maximum degree of the optimal expansion associated with the given set of mean anomaly values. (A finite expansion will be termed "optimal" if it minimizes the root-mean-square (RMS) difference between original and recomputed mean anomaly values.)

A recent investigation[1] concerned with this maximum degree has, using approximate methods, estimated its value for equal area blocks as being 52; this is very close to the actual value of 50 for unequal block sizes, but is too large for equal blocks. The method of determining both the maximum degree and the coefficients themselves is referred to as a collocation, or pseudospectral method[2], or as orthogonal collocation;[3] it will be described presently. (The collocation method described here should not be confused with "least-squares collocation"; see the report of Moritz[4].) In addition, a practical algorithm for determining the surface harmonic expansion which exactly reproduces mean anomaly values will also be given.

Following the development of the exact collocation method will be a discussion concerning the aforementioned approximate methods. Several approximate methods will be detailed, and numerical results stemming from their application will be given. The actual set of mean anomaly values to which these methods are applied will not be given because these values (a particular DMAAC set) are classified, and their inclusion would not permit this report to be approved for public release. The results presented here are independent, however, of the particular set of mean gravity anomaly values used.

HARMONIC ANALYSIS

The gravity anomaly field on the surface of the earth can, in the spherical approximation,[5] be expanded in a series of surface harmonics.[6] In terms of the geocentric latitude φ and longitude λ, this expansion has the form

$$\Delta g\ (\varphi,\lambda) = \sum_{n=0}^{\infty} \sum_{m=0}^{n} P_{nm}\ (\sin\varphi)\ [A_{nm}\ \cos\ m\ \lambda + B_{nm}\ \sin\ m\ \lambda] \qquad (1)$$

The P_{nm} are associated Legendre functions; n is the degree and m is the order of the function (and also of the corresponding term in the expansion). The functions $P_{nm}\ (\sin\varphi)$ $\cos m\ \lambda$ and $P_{nm}(\sin\varphi) \sin m\ \lambda$ are called the surface harmonics of degree n and order m.

The surface harmonics form a complete, orthogonal set of functions on the surface of a sphere. The orthogonality property allows the coefficients of expansion (1) to be determined in the following manner

$$\begin{Bmatrix} A_{nm} \\ B_{nm} \end{Bmatrix} = \frac{2n+1}{4\pi\epsilon_m} \frac{(n-m)!}{(n+m)!} \int_{\varphi=-\frac{\pi}{2}}^{\frac{\pi}{2}} \int_{\lambda=0}^{2\pi} \Delta g(\varphi,\lambda)\, P_{nm}(\sin\varphi) \begin{Bmatrix} \cos m\lambda \\ \sin m\lambda \end{Bmatrix} \cos\varphi\, d\varphi\, d\lambda$$

$$\epsilon_m = \begin{cases} 1, m = 0 \\ \frac{1}{2}, m \neq 0 \end{cases} \qquad (2)$$

MEAN GRAVITY ANOMALIES

Mean gravity anomaly values are obtained by averaging, in a suitable manner, the various point anomaly measurements taken on the terrestrial surface. The averaging is usually done within small blocks into which the surface of the earth has been partitioned; these blocks can be designed to all have approximately the same area[1,7,8,9] or they can be simply demarcated by using a global grid consisting of lines of latitude and longitude. In this latter case (the one specifically considered here) the spacing of the lines need not be uniform; initially, however, it will be assumed that the spacing is uniform and is the same for both lines of latitude and longitude. If this (angular) spacing is denoted by $\bar{\theta}$, then the blocks can be called $\bar{\theta} \times \bar{\theta}$ quadrangles, and the anomalies averaged in them are $\bar{\theta} \times \bar{\theta}$ mean gravity anomalies.

As a concrete example consider the standard case $\bar{\theta} = 5°$. The lines of geocentric latitude are given by

$$\varphi_i = (i - 18)\pi/36 \qquad (i = 0,1,\cdots,35) \qquad (3)$$

and the lines of geocentric longitude by

$$\lambda_j = j\,\pi/36 \qquad (j = 0,1,\cdots,71) \qquad (4)$$

Thus, there are 2592 $5° \times 5°$ quadrangles with 2592 corresponding mean anomaly values $\overline{\Delta g}_{ij}$ (the quadrangle corresponding to $\overline{\Delta g}_{ij}$ is bounded above by φ_{i+1}, below by φ_i, to the east by λ_{j+1} and to the west by λ_j).

ORTHOGONAL COLLOCATION

In order to understand how the value of $\overline{\theta}$ affects the information content of the associated set of mean anomaly values, it is useful to begin with an example involving Fourier series. Suppose a continuous process $f(\theta)$ of period 2π has been sampled at 2N discrete points θ_i, where

$$\theta_i = i\pi/N \qquad (i = 0,1,\cdots, 2N-1) \qquad (5)$$

(Here, $\bar{\theta} = \pi/N$ is the sampling interval.) The Fourier series (of maximum degree $\bar{n}$) which represents $f(\theta)$ is

$$f(\theta) \simeq \sum_{n=0}^{\bar{n}} (a_n \cos n\theta + b_n \sin n\theta) \qquad (6)$$

Consider now the following collocation equations

$$f(\theta_i) = \sum_{n=0}^{\bar{n}} (a_n \cos n\theta_i + b_n \sin n\theta_i) \qquad (i = 0,1,\cdots, 2N-1) \qquad (7)$$

Since i has 2N values, (7) is a set of 2N equations which are linear in the coefficients a_n and b_n. If the last sine coefficient $b_{\bar{n}}$ is excluded from determination, then there are $\bar{n} - 1$ b_n's and $n + 1$ a_n's, for a total of $2\bar{n}$ coefficients. Thus, if $\bar{n} = N$, (7) is a set of 2N linear equations in 2N unknowns and hence can be solved exactly by either matrix inversion or discrete Fourier methods; it is important to note that the coefficients will, in general, be aliased[10]. [The exclusion of $b_{\bar{n}}$ is validated by the fact that $\sin \bar{n}\theta_i = \sin N\theta_i = 0$ for all θ_i in (5).] Since $\bar{\theta} = \pi/N$ and $\bar{n} = N$, the following relation holds between the maximum degree of expansion (6) and the sampling interval $\bar{\theta}$

$$\bar{\theta}\,\bar{n} = \pi \qquad (8)$$

It is easy to carry this result over to double Fourier series: each dimension will have its own sampling interval, and hence its own maximum degree. In particular, if the number of sample points per period in each dimension is the same, then the use of (8) once will yield the maximum degree for both dimensions. This particular result has, of course, been appropriated from the domain of Fourier series to the domain of surface harmonic expansions of mean gravity anomaly fields, where (8) is a well known 'rule of thumb'.[1,7] [The interval $\bar{\theta}$ is equated with the side length of the quadrangle over which the anomalies are averaged. If (6) is averaged over each interval (θ_i, θ_{i+1}), the result is a set of equations similar to (7); therefore, the above considerations still apply. This will be shown in more detail presently.]

Thus, for $\bar{\theta} = 5°$, the relation (8) predicts a maximum degree of $\bar{n} = 36$. This result, however, is valid for Fourier series only and not for surface harmonic expansions. Considerations which lead up to a 'rule of thumb' appropriate for surface harmonic expansions will now be discussed.

SURFACE HARMONIC EXPANSIONS

A finite surface harmonic expansion of the gravity anomaly field is

$$\Delta g_{\bar{n}}(\varphi,\lambda) = \sum_{n=0}^{\bar{n}} \sum_{m=0}^{n} P_{nm}(\sin\varphi)[A_{nm}\cos m\lambda + B_{nm}\sin m\lambda] \tag{9}$$

In order to consider mean gravity anomalies properly, it is necessary to average $\Delta g_{\bar{n}}(\varphi,\lambda)$ over each quadrangle

$$\Delta g_{ij} = \frac{1}{\sigma_{ij}} \int_{\lambda_j}^{\lambda_{j+1}} \int_{\varphi_i}^{\varphi_{i+1}} \Delta g_{\bar{n}}(\varphi,\lambda)\cos\varphi d\varphi d\lambda \tag{10}$$

Here φ_i and λ_j are given by (3) and (4), respectively, and the quadrangle associated with $\overline{\Delta g}_{ij}$ has the area

$$\sigma_{ij} = \int_{\lambda_j}^{\lambda_{j+1}} \int_{\varphi_i}^{\varphi_{i+1}} \cos\varphi d\varphi d\lambda = (\sin\varphi_{i+1} - \sin\varphi_i)(\lambda_{j+1} - \lambda_j) \tag{11}$$

If (9) is now placed into (10), the result is expressible in terms of "weighted" mean anomalies $G_{ij} = \sigma_{ij}\overline{\Delta g}_{ij}$

$$G_{ij} = \sum_{n=0}^{\bar{n}} \sum_{m=0}^{n} D_{nm}^{i} [A_{nm} C_{m}^{j} + B_{nm} S_{m}^{j}] \tag{12}$$

Here the definite integrals of the associated Legendre functions and trigonometric functions are, respectively,

$$D_{nm}^{i} = \int_{\varphi_i}^{\varphi_{i+1}} P_{nm}(\sin\varphi)\cos\varphi d\varphi \tag{13}$$

and

$$C_{m}^{j} = \int_{\lambda_j}^{\lambda_{j+1}} \cos m\lambda d\lambda$$

$$S_{m}^{j} = \int_{\lambda_j}^{\lambda_{j+1}} \sin m\lambda d\lambda \tag{14}$$

The D_{nm}^{i} in (13) can be evaluated using certain recursion relations to be found in Appendix A; the C_{m}^{j} and S_{m}^{j} can be evaluated explicitly

$$C_{0}^{i} = \lambda_{j+1} - \lambda_{j}$$

$$C_{m}^{j} = m^{-1}(\sin m\lambda_{j+1} - \sin m\lambda_{j})$$

$$S_{m}^{j} = m^{-1}(\cos m\lambda_{j} - \cos m\lambda_{j+1}) \qquad (m \neq 0) \tag{15}$$

Consider (12) as a set of collocation equations, similar to those in (7). In order that these equations (12) be solvable exactly, there must be as many coefficients A_{nm} and B_{nm} as there are weighted mean anomalies G_{ij}. (If there are more coefficients than mean anomaly values, the set of equations (12) form an underdetermined linear system. The number of coefficients whose values are uniquely determined is still equal to the number of mean anomaly values; the excess coefficients are essentially arbitrary. In this regard, see Rudin[11].) For the 5° X 5° field considered here, the number of mean gravity anomalies is 2592; since the number of coefficients up to degree $\bar{n}$ is $(\bar{n}+1)^2$, it is necessary to have $\bar{n} = 50$. [Since $(50+1)^2 = 2601$, nine coefficients will have to be excluded from determination. For the case of equal area 5° blocks[1,7,8,9], $\bar{n} \simeq 40$ because the number of blocks is 1654.]

The appropriate rule for finding the maximum degree $\bar{n}$ of a spherical harmonic expansion of $\bar{\theta} \times \bar{\theta}$ mean gravity anomalies can now be expressed. Since the number of coefficients is $(\bar{n}+1)^2$ and the number of mean anomaly values is $2(\pi/\bar{\theta})^2$ [because i has N values and j has 2N values in (12), where $N = \pi/\bar{\theta}$], then these two quantities can be equated to yield the rule

$$\bar{n} \simeq 2^{1/2}\, \pi/\bar{\theta} - 1 \qquad (16)$$

The two sides of (16) are equal only if the right-hand side is an integer; otherwise, $\bar{n}$ is the first integer larger than the right-hand side. [In the general case then, not every coefficient of degree $\bar{n}$ (for example) can be determined. Also, in the revision, I have become aware of a recent result[1,2] which states, essentially, $\bar{n} \simeq 2\,\pi^{1/2}/\bar{\theta}$; (16), however, is the correct result.]

Now, to actually determine the coefficients which allow a set of $\bar{\theta} \times \bar{\theta}$ mean anomalies to be reproduced exactly requires that a set of $2(\pi/\bar{\theta})^2$ linear equations be solved for $2(\pi/\bar{\theta})^2$ unknown coefficients. In the case of $\bar{\theta} = 5°$ this ostensibly requires the inversion of a 2592×2592 matrix, which is impractical on even the largest existing computers. It is possible, however, to construct an algorithm which can circumvent these computational limitations, as long as the constraint of dealing with $\bar{\theta} \times \bar{\theta}$ quadrangles is replaced by a more amenable one. Exactly what is involved in constructing such an algorithm will now be described.

A PRACTICAL ALGORITHM

In the foregoing discussion the lines of latitude and longitude were assigned equal spacings, $\bar{\theta}$; here, there will be no assumptions made as to the spacing of the latitudinal lines, although it will be convenient to keep the longitudinal lines equally spaced. A useful partitioning can be achieved by dividing the surface of the earth into 2M longitudinal sectors and $(M+2)/2$ latitudinal zones (M is even); the intersection of these sectors and zones produces $M(M+2)$ quadrangles. The longitudinal boundaries of these quadrangles are

$$\lambda_j = j\pi/M \qquad (j = 0,1,\cdots,2M-1) \qquad (17)$$

The lines of latitude, though not specifically defined, will be sequentially denoted by φ_i, $i = 0,1,\cdots,M/2$; $\varphi_{i+1} > \varphi_i$. [This, along with (17) insures that (13), (15), and hence (12) are well defined.]

Consider the system of equations given in (12); if the coefficient $A_{\bar{n}\bar{n}}$ is excluded from determination [for essentially the same reason that $b_{\bar{n}}$ in (7) was], then there are a total of $(\bar{n}+1)^2 - 1 = \bar{n}(\bar{n}+2)$ unknown coefficients A_{nm} and B_{nm} in (12). Since the number of quadrangles (and thus mean anomaly values) under consideration is $M(M+2)$, then if $\bar{n} = M$, (12) is a set of $M(M+2)$ linear equations in as many unknowns. Assuming all the equations are independent, (12) can be practically solved by the following method. [The equations must be independent in order that the square matrix which transforms the A_{nm}, B_{nm} into the G_{ij} in (12) posses an inverse. Experience with an essentially identical system of equations shows that this is indeed possible[13].]

In (12) the upper limit on the m-summation can be extended from n to $\bar{n}$ because $P_{nm} = 0$ (and hence $D^i_{nm} = 0$) if $m > n$. Using $\bar{n} = M$, (12) becomes

$$G_{ij} = \sum_{n=0}^{M} \sum_{m=0}^{M} D^i_{nm} (A_{nm} C^j_m + B_{nm} S^j_m) \tag{18}$$

This, in turn can be written as

$$G_{ij} = \sum_{m=0}^{M} (a_{mi} C^j_m + b_{mi} S^j_m) \tag{19}$$

where

$$a_{mi} = \sum_{n=m}^{M} D^i_{nm} A_{nm} \tag{20}$$

$$b_{mi} = \sum_{n=m}^{M} D^j_{nm} B_{nm} \tag{21}$$

The lower limit on the n-summation has been changed by again using the fact that $D^i_{nm} = 0$ for $n < m$. [This particular separation of the latitudinal and longitudinal parts of an equation like (18) has been utilized previously; e.g., cf. Orszag[14].]

Using the relationship $\lambda_{j+1} = \lambda_j + \pi/M$ allows (15) to be written as

$$C^j_0 = \pi/M$$

$$C_m^j = m^{-1}\{\sin(m\pi/M)\cos m\lambda_j - [1 - \cos(m\pi/M)]\sin m\lambda_j\}$$

$$S_m^j = m^{-1}\{[1 - \cos(m\pi/M)]\cos m\lambda_j + \sin(m\pi/M)\sin m\lambda_j\}$$

$$(m \neq 0) \qquad (22)$$

Placing (22) into (18) gives

$$G_{ij} = \frac{a'_{0i}}{2} + \sum_{m-1}^{M-1} (a'_{m\,i}\cos m\lambda_j + b'_{m\,i}\sin m\lambda_j) + \frac{a'_{M\,i}}{2}\cos M\lambda_j \qquad (23)$$

where

$$a'_{0\,i} = 2a_{0\,i}\pi/M$$
$$a'_{M\,i} = 2b_{M\,i}/M$$

$$a'_{m\,i} = m^{-1}\{\sin(m\pi/M)a_{m\,i} + [1 - \cos(m\pi/M)]\,b_{m\,i}\}$$

$$b'_{m\,i} = m^{-1}\{[\cos(m\pi/M) - 1]\,a_{m\,i} + \sin(m\pi/M)b_{m\,i}\}$$

$$(m \neq 0, M) \qquad (24)$$

The set of equations (23) can be solved, for each value of m and i, by standard discrete Fourier methods[10]; the solutions are

$$a'_{m\,i} = M^{-1} \sum_{j=0}^{2M-1} G_{ij}\cos m\lambda_j$$
$$(m = 0,1,\cdots, M;\ i = 0,1,\cdots, M/2)$$

$$b'_{m\,i} = M^{-1} \sum_{j=0}^{2M-1} G_{ij}\sin m\lambda_j$$
$$(m = 1,\cdots, M-1;\ i = 0,1,\cdots, M/2) \qquad (25)$$

Then, the values of the $a_{m\,i}$ and $b_{m\,i}$ can be obtained by inverting the transformation (24)

$$a_{0i} = M\, a'_{0i}/(2\pi)$$

$$b_{Mi} = M\, a'_{Mi}/2$$

$$a_{mi} = \frac{m}{2}\left[\cot\left(\frac{m\pi}{2M}\right) a'_{mi} - b'_{mi}\right]$$

$$b_{mi} = \frac{m}{2}\left[a'_{mi} + \cot\left(\frac{m\pi}{2M}\right) b'_{mi}\right]$$

$$(m \neq 0, M) \qquad (26)$$

The last step is to solve the equations (20) and (21). To do this, (21) will be re-indexed to read

$$b_{M-m,i} = \sum_{n=0}^{m} D^{i}_{M-n,M-m} B_{M-n,M-m} \qquad (27)$$

Then, (20) will be alternately added to and subtracted from (27) to produce

$$b_{M-m,i} \pm a_{mi} = \sum_{n=0}^{m} D^{i}_{M-n,M-m} B_{M-n,M-m} \pm \sum_{n=m}^{M} D^{i}_{nm} A_{nm}$$

$$(m = 0,1,\cdots,M-1;\ i = 0,1,\cdots,M/2) \qquad (28)$$

Since i has $(M+2)/2$ values, (28) is a system of $M+2$ linear equations in $M+2$ unknowns for the values $m = 0,1,\cdots,M-1$. Therefore, (28) can be solved exactly to yield the sought-after $M(M+2)$ coefficients A_{nm} and B_{nm}. (The solution can be achieved by matrix inversion. Again, it is important to note that the coefficients will be aliased, because the gravity anomaly field will, in general, have components whose degree lies beyond M.)

Since the practical algorithm described in this section depends on a particular grid of mean gravity anomalies for its efficacy, such a grid will have to be constructed before any numerical results are forthcoming. If this new partitioning is to contain approximately the same information as the standard $5° \times 5°$ grid, then the value of M required is M = 50. In this case there are 2600 quadrangles with a corresponding set of 2600 mean gravity anomalies; the average angular dimensions of such quadrangles are $6.92° \times 3.6°$ (latitude by longitude).

This algorithm will, for M = 50, break the solution of 2600 linear equations in 2600 unknowns into two parts. First, discrete Fourier methods (25) will be used to solve a system (23) of 26 sets of 100 linear equations in 100 unknowns. Second, matrix inversion will allow for the solution of a system (28) of 50 sets of 52 linear equations in 52 unknowns. Although this is still a lot of work, the problem has at least become tractable.

An advantage of this method is that it produces a surface harmonic expansion which exactly reproduces the mean gravity anomaly values. In contrast, methods for determining coefficients (and hence expansions) by using the orthogonality integrals (2) for surface harmonics can only yield approximate (non-optimal) solutions; these approximate solutions will now be discussed.

ALTERNATIVE DETERMINATION OF COEFFICIENTS

Although the collocation method just described allows the expansion coefficients to be determined optimally (to within numerical round-off error, of course) there also exist alternative methods for determining these coefficients. In particular, the integral (2) can be utilized; since the anomaly data consists of a definite number of mean values, and since the formula (2) requires that the anomaly field be known at ***all*** surface points in order that it yields exact coefficients, it is clear that the use of (2) along with the available data can give rise to, in general, only approximate results. Several methods can be devised to give these approximate coefficients, depending on whether the integral or anomaly field Δg in (2) is approximated; these methods will now be given for the case of $5^\circ \times 5^\circ$ mean anomalies. (It must be stressed that the coefficients determined by orthogonal collocation, though optimal, are also only approximate, in that they are aliased. In the limit $\sigma_{ij} \to 0$, all these methods can be expected to converge to the same result.)

DISCRETE METHODS

First, it will be assumed that the mean anomaly value for a particular quadrangle actually occurs at a specific point within that quadrangle. If this point is arbitrarily chosen to lie at the angular center of the corresponding $(5^\circ \times 5^\circ)$ quadrangle,[9] then (2) must be replaced by a discrete sum such as

$$\begin{Bmatrix} A_{nm} \\ B_{nm} \end{Bmatrix} = \frac{2n+1}{4\pi\epsilon_m} \frac{(n-m)!}{(n+m)!} \sum_{i=1}^{36} \sum_{j-1}^{72} \overline{\Delta g}_{ij} \, P_{nm}(\sin\varphi_i) \begin{Bmatrix} \cos m\lambda_j \\ \sin m\lambda_j \end{Bmatrix} \sigma_{ij}$$

$$\epsilon_m = \begin{cases} 1 & ,m = 0 \\ \frac{1}{2} & ,m \neq 0 \end{cases} \qquad (29)$$

Δg_{ij} : mean anomaly value corresponding to quadrangle containing (φ_i, λ_j)

Here, the quadrangle area σ_{ij} and the positions (φ_i, λ_j) are

$$\begin{aligned} \sigma_{ij} &= \cos \varphi_i \cdot (\pi/36)^2 \\ \varphi_i &= (i - 18.5)\pi/36 \\ \lambda_j &= (j - 0.5)\pi/36 \end{aligned} \tag{30}$$

An alternative method for creating a discrete sum is to use the fact that the actual variables of integration in (2) are $\sin \varphi$ and λ rather than φ and λ; the latter, of course, arise from the former by differentiation: $d(\sin \varphi)d\lambda = \cos \varphi \, d\varphi \, d\lambda$. For this second discrete method, it will be convenient to assume that the anomalies are located (sampled) at that point whose coordinates are the mean values of $\sin \varphi$ and of λ in the corresponding quadrangle. Thus, the summation still has the form (29) and only the quantities in (30) require a partial redefinition

$$\begin{aligned} \sigma_{ij} &= (\sin \varphi_{i+1} - \sin \varphi_i)\pi/36 \\ \sin \varphi_i &= (\sin \varphi_{i+1} + \sin \varphi_i)/2 \\ \lambda_j &= (j - 1/2)\pi/36 \end{aligned} \tag{31}$$

where the upper and lower latitudinal limits are, respectively, $\varphi_{i+1} = \varphi_i + \pi/36$ and $\varphi_i = (i - 18)\pi/36$.

The first discrete method, using (29) and (30), is commonly referred to as "approximation by Riemann sum"; while the second discrete method, using (29) and (31), can be termed "approximation by Riemann-Stieltjes sum".

CONTINUOUS METHODS

In addition to the discrete methods just described, it is also possible to create approximate "continuous" methods. These latter methods use the given set of mean anomaly values to construct a (possibly piecewise) continuous approximation to the surface gravity anomaly field. One example of such an approximation is the "geometrical interpolation"

field found in Heiskanen and Moritz;[15] this construction is a continuous and piecewise linear approximation of the surface anomaly field. Another example is the field which results from assigning to each point of a particular quadrangle the mean anomaly value corresponding to that quadrangle;[7] this field is clearly piecewise-constant (i.e., piecewise-continuous) with a finite number of finite discontinuities. The complexity of the interpolation scheme can obviously be increased to provide many different constructions, all of which give approximate gravity anomaly values anywhere on the surface of the earth.

Any such continuous approximation obviates the use of the discrete formula (29) and allows the integral formula (2) to be used directly in computing the expansion coefficients. Now, although it may appear more elegant to determine coefficients by a continuous rather than a discrete method, there is really no a priori way of deciding which method is actually better. Only by assuming that the interpolation scheme of a particular continuous method correctly describes the behavior of the anomaly field between the "points" at which the anomaly values are known can a continuous method be declared superior to a discrete one.

A fundamentally important quality of all (piecewise) continuous methods is that they assign an anomaly value to every surface point, whereas discrete methods only assign values to a finite number of points. The "sampling interval" for continuous methods is therefore zero, since the "original sampled values" are assumed (whether correctly or not is immaterial) to be known continuously; the corresponding maximum degree is obviously infinite. This optimal property follows from well known results in the theory of orthogonal functions; in particular, from the result that the expansion of a bounded, piecewise-continuous field will always converge "in the square mean"[16] as the degree of the expansion increases toward infinity. ("Square mean" convergence is the continuous analog of the discrete least squares convergence used in the definition of an optimal expansion.) To make these concepts more concrete, the specific case of a "piecewise-constant" continuous method will now be considered.

In the piecewise-constant method of coefficient determination the gravity anomaly field is represented by a multi-valued step function: the anomaly field at every point in a quadrangle is defined to be equal to the corresponding mean value for that quadrangle. The integral formula (2) can therefore be written

$$\begin{Bmatrix} A_{nm} \\ \\ B_{nm} \end{Bmatrix} = \frac{2n+1}{4\pi\,\epsilon_m}\frac{(n-m)!}{(n+m)!}\sum_{i=1}^{36}\sum_{j=1}^{72}\Delta g_{ij}\,D^i_{nm}\begin{Bmatrix} C^i_m \\ \\ S^j_m \end{Bmatrix} \tag{32}$$

where the D^i_{nm}, C^j_m and S^j_m are as described in (13) and (14).

In (32), Δg_{ij} is the mean anomaly value occurring in the quadrangle bounded by the limits

$$\varphi_{i+1} = \varphi_i + \pi/36 \quad , \quad \varphi_i = (i - 18)\pi/36 \qquad (j = 1, \cdots 36)$$

$$\lambda_{j+1} = \lambda_j + \pi/36 \quad , \quad \lambda_j = (j - 1)\pi/36 \qquad (j = 1, \cdots, 72) \quad (33)$$

NUMERICAL RESULTS

Three sets of coefficients were generated from the DMAAC 5° X 5° mean anomaly values by using the two discrete methods and one piecewise-constant (continuous) method. In order to determine the optimal degree of the expansions corresponding to the "discrete" coefficients, and to observe the convergence properties of the expansion corresponding to the "continuous" coefficients, it was necessary to compute how closely these expansions reproduced the original mean anomaly values. Exactly how this was done will now be described.

The "original" gravity anomaly field of the discrete methods consists of a finite number of mean values, each value being assigned to a specific point in the corresponding quadrangle. An appropriate manner for determining how closely these discrete expansions reproduced the original mean values is to compute the weighted root-mean-square (RMS) difference

$$R_n = \left\{ \sum_{i=1}^{36} \sum_{j-1}^{72} \left[\Delta g_N(\varphi_i, \lambda_j) - \overline{\Delta g}_{ij} \right]^2 \frac{\sigma_{ij}}{4\pi} \right\}^{1/2} \qquad (34)$$

Here, $\Delta g_N \ (\varphi_i, \lambda_j)$ is the value of the anomaly field recomputed at the point originally assigned to $\overline{\Delta g}_{ij}$ by using (9) expanded to maximum degree N; the area σ_{ij} is given in (30) for the first discrete method and in (31) for the second discrete method.

The quantities R_N were determined for the expansions produced by both the first and second discrete methods for N = 0, 1, $\cdots$, 81. The numerical results for these two methods were practically identical with one another; therefore, only the results for the first method will be presented in graphical form (see Figure 1). The actual values of the R_N for both methods, as well as the maximum difference between the original and recomputed anomaly values, are given in Tables B-1 and B-2 of Appendix B.

In the case of the piecewise-constant method, the "closeness" of the expansion (9) could be measured by the RMS integral [analogous to the sum (34)]

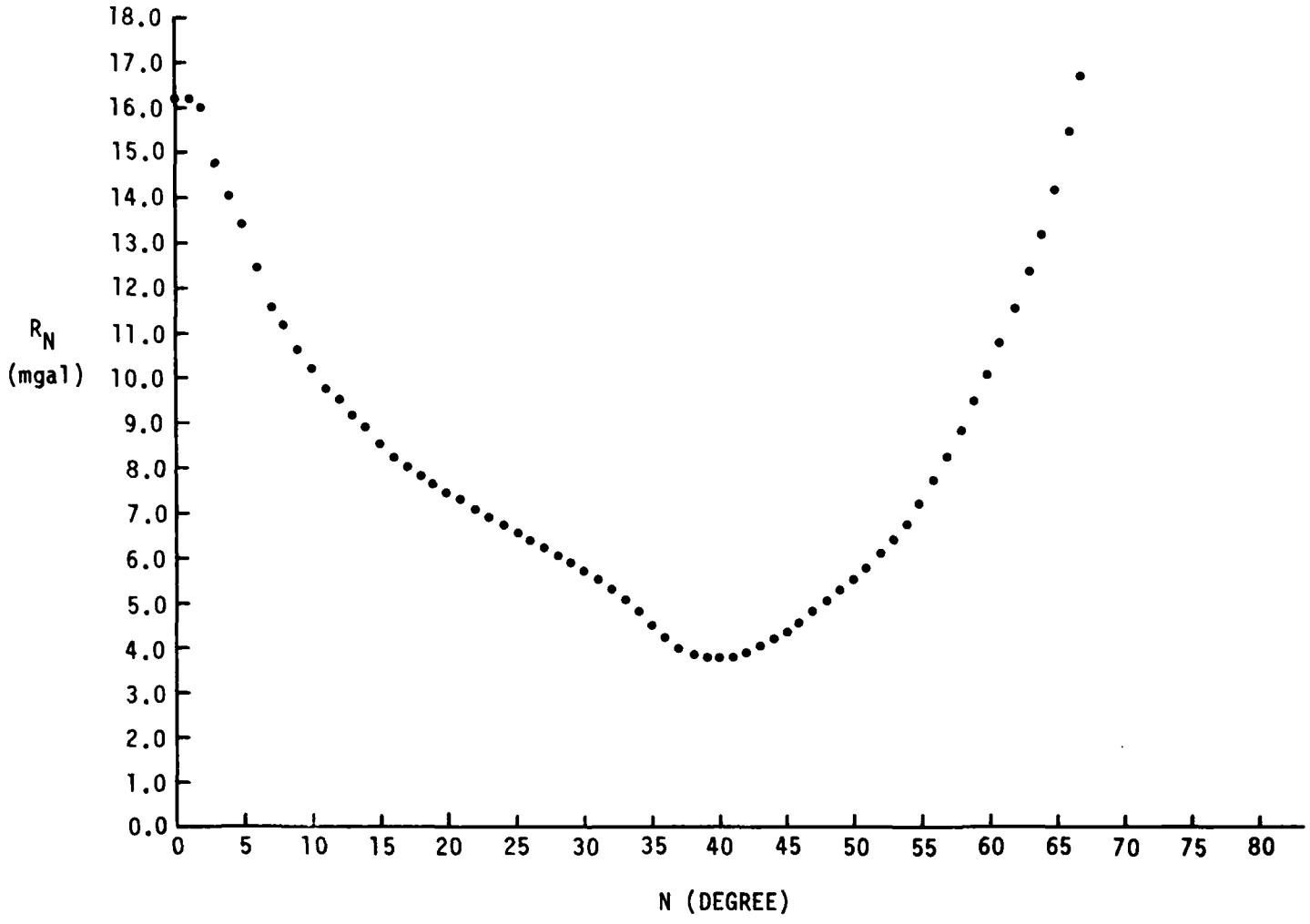

Figure 1. RMS Differences From Using First Discrete Method Coefficients to Recompute Point Anomaly Values.

$$R_N = \left\{ \frac{1}{4\pi} \int_{\lambda=0}^{2\pi} \int_{\varphi=-\pi/2}^{\pi/2} [\Delta g_N(\varphi, \lambda) - \overline{\Delta g}]^2 \cos\varphi d\varphi d\lambda \right\}^{1/2} \tag{35}$$

(Here $\overline{\Delta g}$ is the "original" anomaly field which was attained by assigning to all points in a particular quadrangle the mean anomaly value corresponding to that quadrangle.) The result of applying (35) is a foregone conclusion; however, it is the root of the previously mentioned "square mean" which always converges as $N \to \infty$.

Although the convergence of (35) is well established, it would still be useful to see just how well the expansion (9) with the coefficients generated by the piecewise-constant method does converge. An appropriate way is to first average the results of (9) within each quadrangle [as is done in (10)]

$$\overline{\Delta g}_{N,ij} = \frac{1}{\sigma_{ij}} \int_{\lambda_j}^{\lambda_{j+1}} \int_{\varphi_i}^{\varphi_{i+1}} \Delta g_N(\varphi, \lambda) \cos\varphi d\varphi d\lambda \tag{36}$$

Using (9), (13) and (14) gives

$$\overline{\Delta g}_{N,ij} = \frac{1}{\sigma_{ij}} \sum_{n=0}^{N} \sum_{m=0}^{N} D_{nm}^{i} \left(A_{nm} C_m^j + B_{nm} S_m^j \right) \tag{37}$$

Finally, an RMS difference similar to (34) can be defined

$$R_N = \left[\sum_{i=1}^{36} \sum_{j=1}^{72} (\overline{\Delta g}_{N,ij} - \overline{\Delta g}_{ij})^2 \frac{\sigma_{ij}}{4\pi} \right]^{1/2} \tag{38}$$

Computed values of R_N for N = 0, 1,$\cdots$,81 are graphed in Figure 2; the numerical values of R_N and the maximum differences between original and recomputed mean anomalies are listed in Table B-3 of Appendix B.

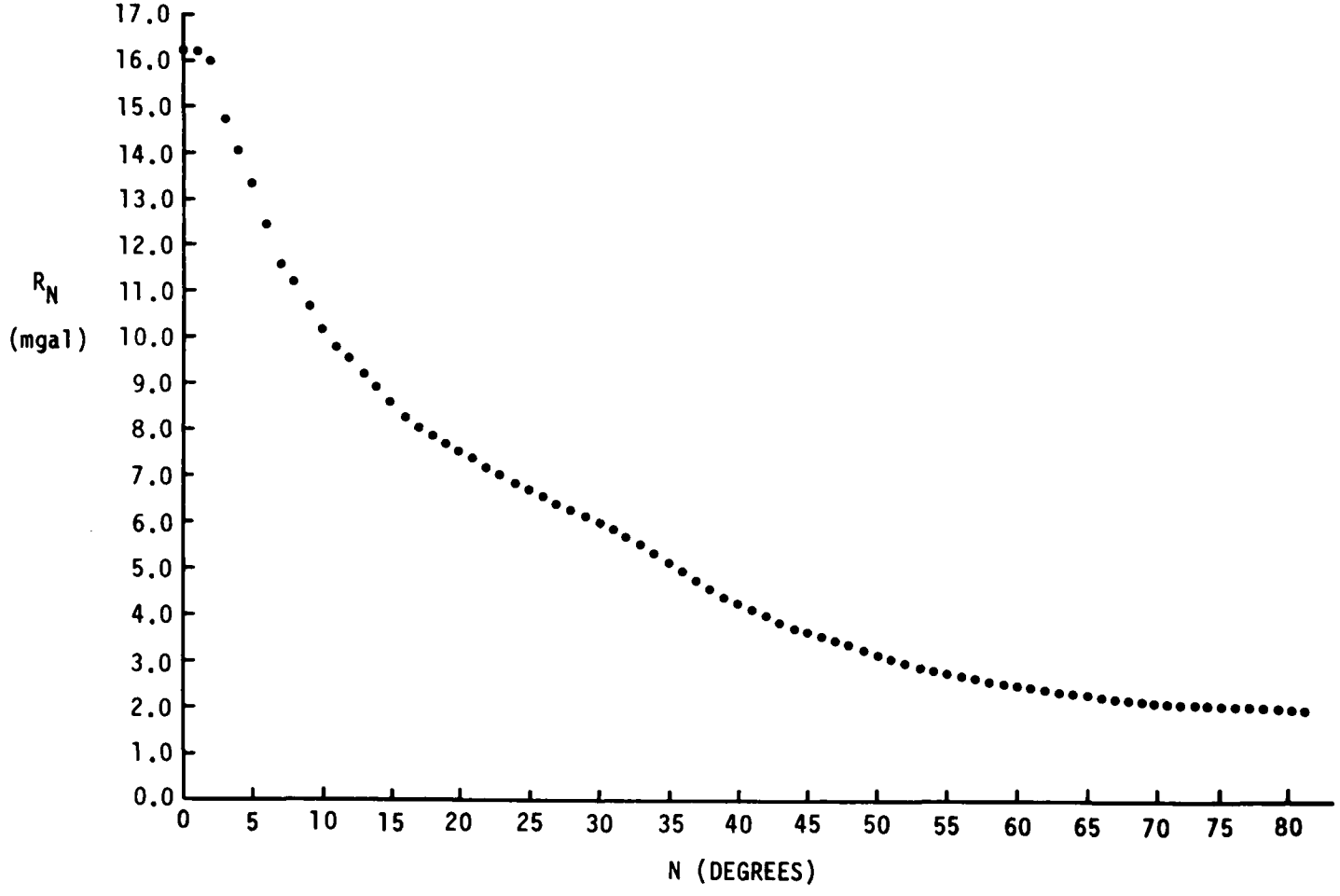

Figure 2. RMS Differences From Using Piecewise-Constant Method Coefficients to Recompute Quadrangle Averaged Anomaly Values

ADDITIONAL CONSIDERATIONS

Since the apparatus for averaging surface harmonic expansions over quadrangles and comparing these averaged anomalies with the original set of mean anomalies has already been established [by (10), (37) and (38)], it may be of interest to apply this apparatus to expansions which use "discrete" coefficients. It might be expected that the effects of terms of high degree would, more or less, be averaged out, and that the extremely divergent behavior shown in Figure 1 would be attenuated. That this is indeed the case is shown in Figure 3; the results graphed there come from using the coefficients generated by the first discrete method in conjunction with (37) and (38). The results obtained by using the coefficients generated by the second discrete method are almost identical with those of the first; the results from both the first and second discrete methods are given in Tables B-4 and B-5 of Appendix B.

Although the apparatus of quadrangle averaging (37) and averaged anomaly comparison (38) provides an appropriate means for studying the convergence of expansions generated by use of the piecewise-constant method, it is informative to investigate the ***pointwise*** convergence of these same expansions. In general, the convergence of an orthoganal expansion of a given function at a specific point does not automatically follow from the fact that the expansion converges to the function "in the square mean" (in fact, there are functions which converge in the square mean and yet fail to converge at ***any*** specific point[15]). If the function being expanded, however, is reasonably well behaved, its pointwise convergence is certainly not precluded; in particular, if S[f] is the Fourier expansion of a function f then, "If f is of bounded variation, S[f] converges uniformly at every point of continuity of f".[17] (At points of finite discontinuity f shows "Gibbs' phenomenon"[18].) Similarly, if a function continuous on a closed interval is expanded in a series of Legendre polynomials, the Weierstrass approximation theorem[19] implies that this series of polynomials converges uniformly to the function; if the function is only piecewise-continuous, Gibbs' phenomenon again appears at the points of (finite) discontinuity[20].

In the case of a surface harmonic expansion of a piecewise-constant function, the Stone-Weierstrass theorem[21] implies uniform convergence everywhere except for arbitrarily small neighborhoods about the points of discontinuity. Expropriating the results concerning the behavior of Fourier and Legendre series at points of discontinuity, it is reasonable to assume that series of surface harmonics show analogous behavior at such points. Thus, if the coefficients generated by the piecewise-constant method are used in (9) to compute anomaly values at the angular centers (for example) of the quadrangles, it is expected that the RMS difference (34) will show convergence as $N \rightarrow \infty$. The actual results for this procedure are shown in Figure 4; the convergence, though not as smooth as in Figure 2, is indicated (a decreasing sequence of relative maxima may be expected to exist as $N \rightarrow \infty$). The numerical values from which Figure 4 is derived are to be found in Table B-6 of Appendix B.

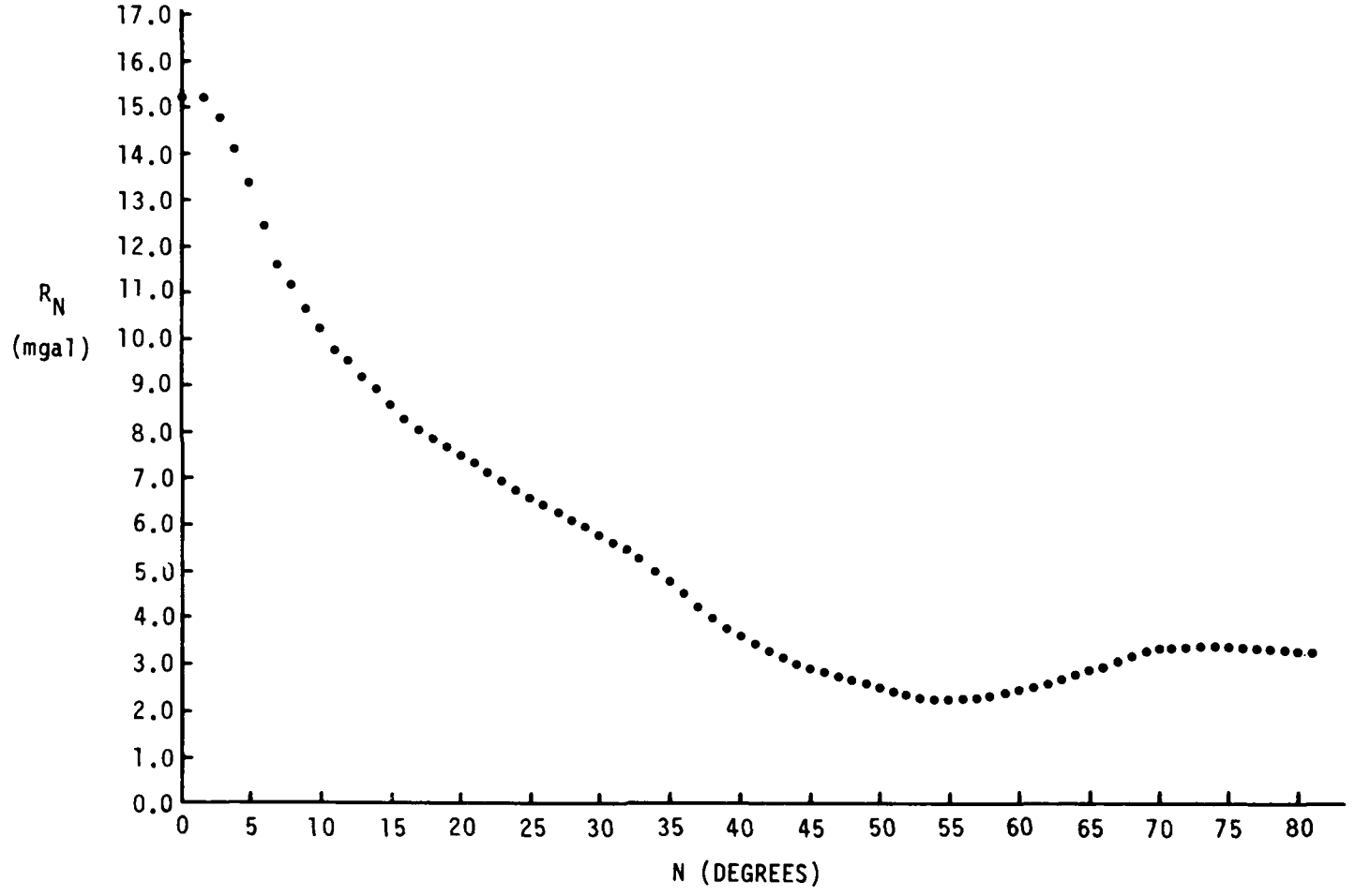

Figure 3. RMS Differences From Using First Discrete Method Coefficients to Recompute Quadrangle Averaged Anomaly Values.

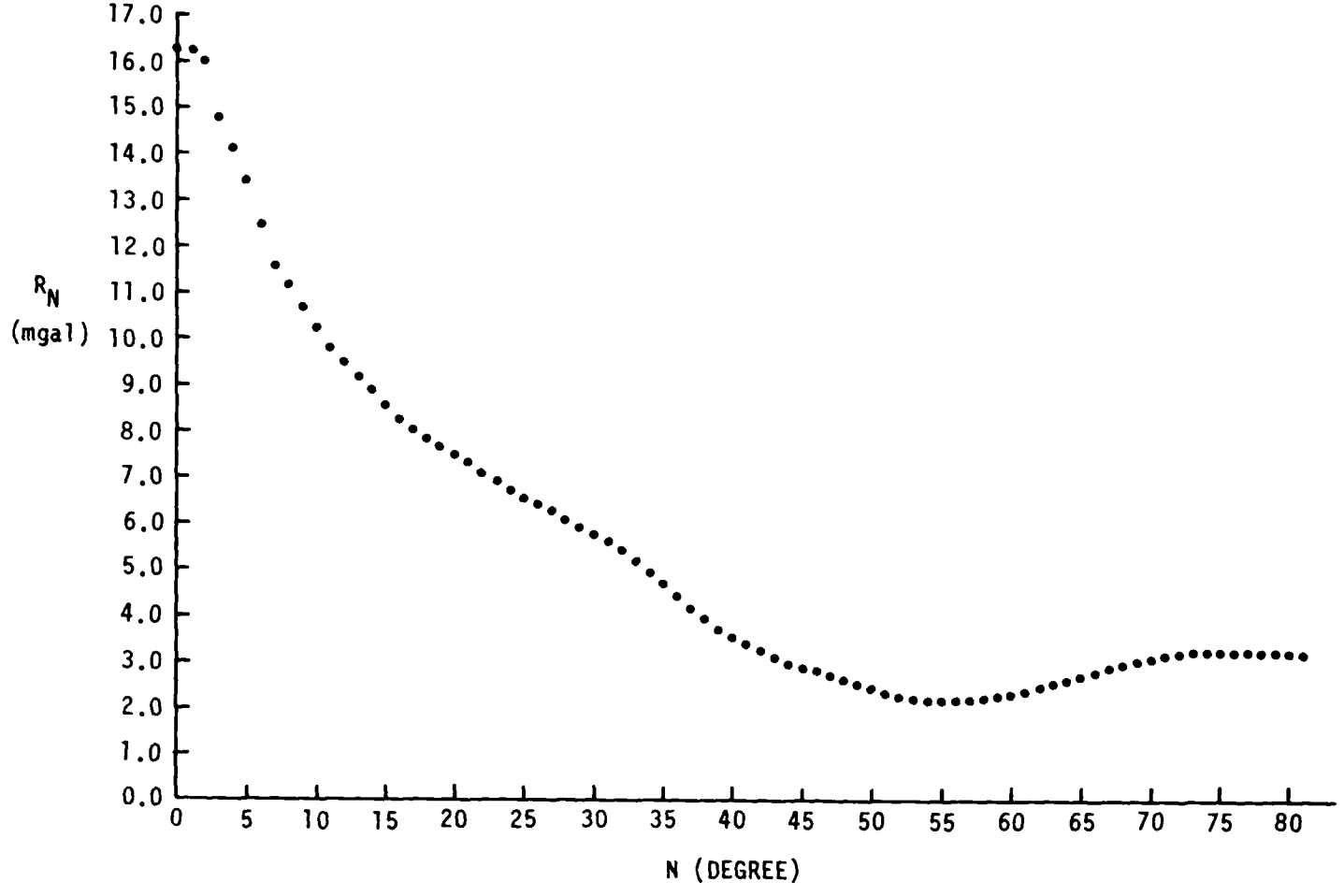

Figure 4. RMS Difference From Using Piecewise-Constant Method Coefficients to Recompute Point Anomaly Values

CONCLUSIONS

The material presented in this report has included a new method for determining the surface harmonic expansion coefficients for the terrestrial gravity anomaly field (and hence the coefficients of the geopotential[22]). This method requires a particular partitioning of the earth's surface into quadrangles and therefore must have a set of mean anomalies which correspond to this new partitioning. Since such a set does not presently exist, the application of this method must await its creation.

In conjunction with this new (collocation) method, alternative methods for coefficient determination were also discussed. These alternative methods have an advantage over the collocation method in that they do not depend on a particular partitioning grid on the earth's surface in order to be practical. Also, they can be expected to produce reasonably accurate values for coefficients of low degree.

The collocation method, in turn, has an advantage over these alternative methods since it can produce an expansion which matches the original mean anomalies exactly (in theory). (This is not to say that the expansion coefficients are exact; this possibility is generally obviated by aliasing.) The exact nature of a solution by collocation also allows the maximum degree of an expansion corresponding to a given set of mean gravity anomalies to be precisely determined, whereas these alternative methods can only provide rough estimates.

REFERENCES

1. R. H. Rapp, "The Relationship Between Mean Anomaly Block Sizes and Spherical Harmonic Representations", *J. Geophys. Res.*,**82**, 5360-5364,1977.

2. D. Gottlieb and S. A. Orszag, ***Numerical Analysis of Spectral Methods: Theory and Application***, pp, 13-17, SIAM, Philadelphia, 1977.

3. J. P. Boyd, "The Choice of Spectral Methods on a Sphere for Boundary and Eigenvalue Problems: A Comparison of Chebyshev, Fourier and Associated Legendre Functions," *Mon. Wea. Rev., 106*, 1184-1191, 1978.

4. H. Mortiz, ***Advanced Least-Squares Methods,*** Rep. No. 175, Dept. of Geod. Sci., Ohio State, Columbus, OH, 1972.

5. W. A. Heiskanen and H. Moritz, ***Physical Geodesy***, Sec. 2-14, Freeman, San Francisco, 1967.

6. Ref. 5, 2-20.

7. R. H. Rapp, ***Potential Coefficient Determinations from 5° Terrestrial Gravity Data***, Report 251, Dept. of Geod. Sci., Ohio State, Columbus, Ohio, 1977.

8. M. R. Williamson and E. M. Gaposchkin, ***The Estimation of 550 Km X 550 km Mean Gravity Anomalies***, Special Report 363, Smithsonian Institution Astrophysical Observatory, Cambridge, MA, 1975.

9. W. J. Rothermel, et. al., *A **Global Gravity Model Based Entirely Upon Terrestrial Data (Globgrav III)***, DMAAC/TR-76-003, Defense Mapping Agency Aerospace Center, St. Louis Air Force Station, MO, 1976. CONFIDENTIAL

10. R. W. Hamming, ***Numerical Methods for Scientists and Engineers, pp. 67-69;176-278, McGraw-Hill, New York, NY, 1962.***

11. W. Rudin, ***Principles of Mathematical Analysis,*** 2nd Ed., p. 195: "The Implicit Function Theorem," McGraw-Hill, New York, NY, 1964.

12. F. J. Lowes, "Comment on 'The Relationship Between Mean Anomaly Block Size and Spherical Harmonic Representations' by Richard H. Rapp", *J. Geophys. Res., 84,* 4781-4782, 1979.

13. J. V. Shebalin, ***On the Theory and Optimization of Global Point-Mass Expansions of Anomalous Gravity***, pp. 22-23, TR 79-170, NSWC, Dahlgren, VA, 1979.

14. S. A. Orszag, "Fourier Series on Spheres," Sec 2.v, ***Mon. Wea. Rev, 102***, 56-75, 1974.

15. Ref. 5, Sec. 7-5.

16. J. Dieudonne, ***Treatise on Analysis***, Vol. 2, pp. 151-157, Academic Press, New York, 1970.

17. A. Zygmund, ***Trigonometric Series***, Vol. 1, P. 58, Cambridge, UK, 1968.

18. Ref. 15, p. 61.

19. Ref. 11, p. 146.

20. Ref. 2, pp. 37-40.

21. Ref. 11, pp. 146-153.

22. Ref. 5, pp. 108-109.

23. G. Arfken, ***Mathematical Methods for Physicists***, 2nd Ed., p. 560, Academic Press, New York, 1970.

24. M. K. Paul, "Recurrence Relations for Integrals of Associated Legendre Functions", ***Bulletin Geodesique, 52***, 3, pp 177-190, 1978.

APPENDIX A

Recursion Relations for Definite Integrals of Associated Legendre Functions

The definite integral of an associated Legendre function

$$D^i_{nm} = \int_{\varphi_i}^{\varphi_{i+1}} P_{nm}(\sin\varphi)\cos\varphi \, d\varphi \tag{39}$$

can be evaluated through the use of recursion relations. Using the well known recursion relations of the associated Legendre functions themselves[23] allows the following recursion relations for the D^i_{nm} to be easily derived

$$D^i_{no} = (2n+1)^{-1}(R^i_{o,n+1,o} - R^i_{o,n-1,o})$$

$$D^i_{n,m+1} = (m-1)^{-1}\left\{2mR^i_{1,nm} + (m+1)[n(n+1) - m(m-1)]D^i_{n,m-1}\right\}$$

$$D^i_{n+1,m}, = [(n-m+1)(n+2)]^{-1}\left\{(n+m)(n-1)D^i_{n-1,m} - 3^{-1}(2n+1)R^i_{2,nm}\right\} \tag{40}$$

Here

$$R^i_{k,nm} = P_{kk}(x)P_{nm}(x)\Big|_{\sin\varphi_i}^{\sin\varphi_{i+1}} \tag{41}$$

and

$$F(y)\Big|_{z_1}^{z_2} = F(z_2) - F(z_1) \tag{42}$$

For numerical application it is useful to have the following

$$D^i_{00} = \sin\varphi \Big|_{\varphi_i}^{\varphi_{i+1}}$$

$$D^i_{10} = 1/2 \sin^2\varphi \Big|_{\varphi_i}^{\varphi_{i+1}}$$

$$D^i_{11} = 1/2 (\varphi + \sin\varphi \cos\varphi) \Big|_{\varphi_i}^{\varphi_{i+1}}$$

$$D^i_{20} = - 1/2 \sin\varphi \cos^2\varphi \Big|_{\varphi_i}^{\varphi_{i+1}}$$

$$D^i_{21} = - \cos^3\varphi \Big|_{\varphi_i}^{\varphi_{i+1}}$$

$$D^i_{22} = \sin\varphi(3 - \sin^2\varphi) \Big|_{\varphi_i}^{\varphi_{i+1}}$$

$$D^i_{32} = - \frac{15}{4} \cos^4\varphi \Big|_{\varphi_i}^{\varphi_{i+1}} \qquad (43)$$

The combination of (40), (41) and (43) is sufficient to generate the D^i_{nm} to any desired degree and order.

(In the review process I have become aware of prior sources for these results, both published and unpublished; for example, see the article by Paul[24].)

APPENDIX B

Numerical Results

The numerical results presented in the following six tables consist of values of the three quantitities N, R_N, and M_N, where

N:	degree of the expansion
R_N:	RMS difference between original anomalies and anomalies recomputed by using an expansion of degree N
M_N:	Maximum difference between original anomalies and anomalies recomputed by using an expansion of degree N.

Table B-1. Numerical Results Generated by Using First Discrete Method With R_N From (15).

0	.1626E+02	.8910E+02	28	.6012E+01	.3674E+02	55	.7175E+01	.4358E+02
1	.1626E+02	.8910E+02	29	.5952E+01	.3696E+02	56	.7700E+01	.4369E+02
2	.1600E+02	.9114E+02	30	.5682E+01	.3809E+02	57	.8201E+01	.4566E+02
3	.1475E+02	.8798E+02	31	.5495E+01	.3623E+02	58	.8761E+01	.4738E+02
4	.1405E+02	.8022E+02	32	.5290E+01	.3541E+02	59	.9473E+01	.5113E+02
5	.1336E+02	.8317E+02	33	.5050E+01	.3345E+02	60	.1004E+02	.5008E+02
6	.1243E+02	.8059E+02	34	.4744E+01	.3176E+02	61	.1075E+02	.5034E+02
7	.1154E+02	.7182E+02	35	.4491E+01	.3011E+02	62	.1154E+02	.5198E+02
8	.1119E+02	.7360E+02	36	.4207E+01	.2733E+02	63	.1231E+02	.7079E+02
9	.1065E+02	.6618E+02	37	.3956E+01	.2585E+02	64	.1314E+02	.7500E+02
10	.1019E+02	.6588E+02	38	.3826E+01	.2685E+02	65	.1416E+02	.8387E+02
11	.9745E+01	.5999E+02	39	.3724E+01	.2481E+02	66	.1542E+02	.9092E+02
12	.9526E+01	.6395E+02	40	.3763E+01	.2590E+02	67	.1666E+02	.9997E+02
13	.9154E+01	.6251E+02	41	.3793E+01	.2434E+02	69	.1858E+02	.1154E+03
14	.8902E+01	.5671E+02	42	.3964E+01	.2513E+02	69	.2107E+02	.1242E+03
15	.8540E+01	.5662E+02	43	.4046E+01	.2537E+02	70	.2270E+02	.1425E+03
16	.8212E+01	.5274E+02	44	.4188E+01	.2718E+02	71	.2493E+02	.1581E+03
17	.7986E+01	.5233E+02	45	.4330E+01	.2536E+02	72	.2707E+02	.1514E+03
18	.7820E+01	.4887E+02	46	.4488E+01	.2537E+02	73	.3084E+02	.1795E+03
19	.7631E+01	.4770E+02	47	.4805E+01	.2633E+02	74	.3322E+02	.1958E+03
20	.7469E+01	.4734E+02	48	.5016E+01	.2846E+02	75	.3659E+02	.2068E+03
21	.7307E+01	.4704E+02	49	.5240E+01	.3093E+02	76	.3928E+02	.2174E+03
22	.7062E+01	.4239E+02	50	.5508E+01	.3395E+02	77	.4104E+02	.2279E+03
23	.6869E+01	.3964E+02	51	.5712E+01	.3726E+02	78	.4266E+02	.2309E+03
24	.6681E+01	.3787E+02	52	.6056E+01	.3869E+02	79	.4422E+02	.2497E+03
25	.6506E+01	.3577E+02	53	.6389E+01	.4183E+02	80	.4559E+02	.2457E+03
26	.6386E+01	.3446E+02	54	.6691E+01	.4051E+02	81	.4670E+02	.2561E+03
27	.6211E+01	.3384E+02						

Table B-2. Numerical Results Generated by Using Second Discrete Method With R_N From(15).

0	.1626E+02	.8910E+02	28	.6012E+01	.3670E+02	55	.7151E+01	.4347E+02
1	.1626E+02	.8910E+02	29	.5853E+01	.3703E+02	56	.7673E+01	.4362E+02
2	.1600E+02	.9114E+02	30	.5684E+01	.3811E+02	57	.8167E+01	.4571E+02
3	.1475E+02	.8799E+02	31	.5495E+01	.3613E+02	58	.8746E+01	.4736E+02
4	.1405E+02	.8021E+02	32	.5298E+01	.3540E+02	59	.9438E+01	.5127E+02
5	.1337E+02	.8316E+02	33	.5051E+01	.3345E+02	60	.1000E+02	.5610E+02
6	.1243E+02	.8056E+02	34	.4745E+01	.3170E+02	61	.1068E+02	.6013E+02
7	.1154E+02	.7181E+02	35	.4489E+01	.3018E+02	62	.1147E+02	.6193E+02
8	.1119E+02	.7359E+02	36	.4202E+01	.2733E+02	63	.1221E+02	.7072E+02
9	.1065E+02	.6620E+02	37	.3951E+01	.2563E+02	64	.1304E+02	.7475E+02
10	.1019E+02	.6591E+02	38	.3818E+01	.2648E+02	65	.1410E+02	.8390E+02
11	.9744E+01	.5994E+02	39	.3711E+01	.2452E+02	66	.1535E+02	.9082E+02
12	.9526E+01	.6389E+02	40	.3750E+01	.2457E+02	67	.1654E+02	.9962E+02
13	.9155E+01	.6249E+02	41	.3777E+01	.2407E+02	68	.1846E+02	.1147E+03
14	.8903E+01	.5673E+02	42	.3849E+01	.2482E+02	69	.2088E+02	.1285E+03
15	.8544E+01	.5663E+02	43	.4034E+01	.2496E+02	70	.2249E+02	.1423E+03
16	.8214E+01	.5272E+02	44	.4174E+01	.2539E+02	71	.2474E+02	.1577E+03
17	.7985E+01	.5230E+02	45	.4317E+01	.2511E+02	72	.2685E+02	.1609E+03
18	.7821E+01	.4882E+02	46	.4476E+01	.2521E+02	73	.3047E+02	.1791E+03
19	.7631E+01	.4778E+02	47	.4790E+01	.2607E+02	74	.3285E+02	.1941E+03
20	.7470E+01	.4735E+02	48	.5002E+01	.2644E+02	75	.3638E+02	.2053E+03
21	.7308E+01	.4700E+02	49	.5225E+01	.3082E+02	76	.3912E+02	.2172E+03
22	.7063E+01	.4235E+02	50	.5481E+01	.3379E+02	77	.4091E+02	.2277E+03
23	.6870E+01	.3961E+02	51	.5694E+01	.3726E+02	78	.4256E+02	.2307E+03
24	.6681E+01	.3783E+02	52	.6038E+01	.3863E+02	79	.4414E+02	.2454E+03
25	.6507E+01	.3571E+02	53	.6368E+01	.4193E+02	80	.4550E+02	.2456E+03
26	.6307E+01	.3446E+02	54	.6672E+01	.4051E+02	81	.4660E+02	.2578E+03
27	.6211E+01	.3380E+02						

Table B-3. Numerical Results Generated by Using Piecewise-Constant Method With R_N From (19).

0	.1626E+02	.8910E+02	28	.6228E+01	.3776E+02	55	.2761E+01	.2543E+02
1	.1626E+02	.8910E+02	29	.6100E+01	.3808E+02	56	.2691E+01	.2514E+02
2	.1680E+02	.9113E+02	30	.5964E+01	.3867E+02	57	.2622E+01	.2499E+02
3	.1475E+02	.8800E+02	31	.5817E+01	.3757E+02	58	.2571E+01	.2490E+02
4	.1405E+02	.8032E+02	32	.5667E+01	.3702E+02	59	.2514E+01	.2489E+02
5	.1337E+02	.8322E+02	33	.5497E+01	.3588E+02	60	.2472E+01	.2423E+02
6	.1243E+02	.8069E+02	34	.5285E+01	.3500E+02	61	.2428E+01	.2438E+02
7	.1154E+02	.7221E+02	35	.5118E+01	.3417E+02	62	.2382E+01	.2416E+02
8	.1119E+02	.7389E+02	36	.4912E+01	.3270E+02	63	.2343E+01	.2383E+02
9	.1065E+02	.6686E+02	37	.4708E+01	.3120E+02	64	.2311E+01	.2396E+02
10	.1019E+02	.6657E+02	38	.4535E+01	.3063E+02	65	.2282E+01	.2404E+02
11	.9752E+01	.6110E+02	39	.4355E+01	.2878E+02	66	.2250E+01	.2374E+02
12	.9535E+01	.6474E+02	40	.4234E+01	.2980E+02	67	.2215E+01	.2372E+02
13	.9168E+01	.6346E+02	41	.4107E+01	.2777E+02	68	.2192E+01	.2379E+02
14	.8920E+01	.5833E+02	42	.3959E+01	.2639E+02	69	.2166E+01	.2348E+02
15	.8567E+01	.5824E+02	43	.3834E+01	.2584E+02	70	.2145E+01	.2306E+02
16	.8244E+01	.5493E+02	44	.3710E+01	.2502E+02	71	.2124E+01	.2296E+02
17	.8024E+01	.5456E+02	45	.3609E+01	.2529E+02	72	.2100E+01	.2256E+02
18	.7865E+01	.5171E+02	46	.3542E+01	.2465E+02	73	.2084E+01	.2229E+02
19	.7684E+01	.5080E+02	47	.3412E+01	.2441E+02	74	.2068E+01	.2199E+02
20	.7531E+01	.5053E+02	48	.3330E+01	.2415E+02	75	.2052E+01	.2156E+02
21	.7381E+01	.5029E+02	49	.3235E+01	.2485E+02	76	.2037E+01	.2125E+02
22	.7153E+01	.4680E+02	50	.3137E+01	.2543E+02	77	.2022E+01	.2105E+02
23	.6976E+01	.4479E+02	51	.3053E+01	.2609E+02	78	.2007E+01	.2088E+02
24	.6805E+01	.4348E+02	52	.2955E+01	.2553E+02	79	.1994E+01	.2048E+02
25	.6649E+01	.4009E+02	53	.2875E+01	.2516E+02	80	.1981E+01	.2028E+02
26	.6544E+01	.3878E+02	54	.2816E+01	.2488E+02	81	.1969E+01	.2014E+02
27	.6394E+01	.3738E+02						

Table B-4. Numerical Results Generated by Using First Discrete Method With R_N From (19).

0	.1626E+02	.8918E+02	28	.6875E+01	.3728E+02	55	.2273E+01	.2769E+02
1	.1526E+02	.8910E+02	29	.5928E+01	.3747E+02	56	.2279E+01	.2699E+02
2	.1600E+02	.9113E+02	30	.5778E+01	.3837E+02	57	.2271E+01	.2689E+02
3	.1475E+02	.8799E+02	31	.5592E+01	.3690E+02	58	.2322E+01	.2691E+02
4	.1405E+02	.8027E+02	32	.5+07E+01	.3623E+02	59	.2394E+01	.2379E+02
5	.1337E+02	.8320E+02	33	.5195E+01	.3476E+02	60	.2439E+01	.2494E+02
6	.1243E+02	.8063E+02	34	.4324E+01	.3347E+02	61	.2476E+01	.2684E+02
7	.1154E+02	.7201E+02	35	.4702E+01	.3232E+02	62	.2565E+01	.2589E+02
8	.1119E+02	.7375E+02	36	.4431E+01	.3026E+02	63	.2663E+01	.2448E+02
9	.1065E+02	.6652E+02	37	.4157E+01	.2804E+02	64	.2745E+01	.2580E+02
10	.1019E+02	.6623E+02	38	.3936E+01	.2726E+02	65	.2813E+01	.2750E+02
11	.9746E+01	.6057E+02	39	.3708E+01	.2439E+02	66	.2890E+01	.2534E+02
12	.9529E+01	.6435E+02	40	.3573E+01	.2496E+02	67	.3019E+01	.2643E+02
13	.9159E+01	.6297E+02	41	.3424E+01	.2392E+02	68	.3116E+01	.3080E+02
14	.8909E+01	.5752E+02	42	.3245E+01	.2430E+02	69	.3239E+01	.4142E+02
15	.8551E+01	.5742E+02	43	.3124E+01	.2452E+02	70	.3297E+01	.4255E+02
16	.8222E+01	.5384E+02	44	.2989E+01	.2557E+02	71	.3291E+01	.3197E+02
17	.7997E+01	.5345E+02	45	.2880E+01	.2506E+02	72	.3336E+01	.3011E+02
18	.7934E+01	.5032E+02	46	.2823E+01	.2499E+02	73	.3364E+01	.3526E+02
19	.7647E+01	.4326E+02	47	.2713E+01	.2464E+02	74	.3379E+01	.3361E+02
20	.7488E+01	.4894E+02	48	.2645E+01	.2415E+02	75	.3370E+01	.2525E+02
21	.7330E+01	.4867E+02	49	.2557E+01	.2543E+02	76	.3344E+01	.2826E+02
22	.7090E+01	.4465E+02	50	.2467E+01	.2717E+02	77	.3330E+01	.2274E+02
23	.6901E+01	.4230E+02	51	.2383E+01	.2869E+02	78	.3324E+01	.2321E+02
24	.5718E+01	.4083E+02	52	.2301E+01	.2740E+02	79	.3306E+01	.2277E+02
25	.6549E+01	.3670E+02	53	.2255E+01	.2607E+02	80	.3291E+01	.2322E+02
26	.6432E+01	.3632E+02	54	.2242E+01	.2564E+02	81	.3272E+01	.2279E+02
27	.6264E+01	.3499E+02						

Table B-5. Numerical Results Generated by Using Second Discrete Method With R_N From (19).

0	.1626E+02	.8910E+02	28	.6075E+01	.3733E+02	55	.2265E+01	.2778E+02
1	.1626E+02	.8910E+02	29	.5928E+01	.3760E+02	56	.2272E+01	.2723E+02
2	.1600E+02	.9114E+02	30	.5771E+01	.3847E+02	57	.2263E+01	.2695E+02
3	.1475E+02	.8799E+02	31	.5592E+01	.3693E+02	58	.2315E+01	.2707E+02
4	.1405E+02	.8027E+02	32	.5407E+01	.3633E+02	59	.2389E+01	.2393E+02
5	.1337E+02	.8318E+02	33	.5195E+01	.3486E+02	60	.2429E+01	.2509E+02
6	.1243E+02	.8062E+02	34	.4923E+01	.3354E+02	61	.2479E+01	.2697E+02
7	.1154E+02	.7201E+02	35	.4701E+01	.3246E+02	62	.2564E+01	.2598E+02
8	.1119E+02	.7375E+02	36	.4429E+01	.3039E+02	63	.2664E+01	.2462E+02
9	.1065E+02	.6655E+02	37	.4156E+01	.2812E+02	64	.2739E+01	.2587E+02
10	.1019E+02	.6626E+02	38	.3934E+01	.2740E+02	65	.2807E+01	.2759E+02
11	.9746E+01	.6052E+02	39	.3706E+01	.2453E+02	66	.2888E+01	.2542E+02
12	.9529E+01	.6429E+02	40	.3571E+01	.2493E+02	67	.3011E+01	.2690E+02
13	.9159E+01	.6295E+02	41	.3421E+01	.2362E+02	68	.3108E+01	.3066E+02
14	.8909E+01	.5754E+02	42	.3242E+01	.2396E+02	69	.3221E+01	.4171E+02
15	.8551E+01	.5744E+02	43	.3121E+01	.2438E+02	70	.3280E+01	.4231E+02
16	.8222E+01	.5395E+02	44	.2987E+01	.2488E+02	71	.3270E+01	.2941E+02
17	.7937E+01	.5346E+02	45	.2877E+01	.2505E+02	72	.3312E+01	.2772E+02
18	.7835E+01	.5032E+02	46	.2820E+01	.2498E+02	73	.3357E+01	.3702E+02
19	.7647E+01	.4932E+02	47	.2710E+01	.2477E+02	74	.3375E+01	.3573E+02
20	.7488E+01	.4900E+02	48	.2641E+01	.2432E+02	75	.3362E+01	.2552E+02
21	.7330E+01	.4869E+02	49	.2552E+01	.2574E+02	76	.3334E+01	.2677E+02
22	.7090E+01	.4467E+02	50	.2462E+01	.2747E+02	77	.3318E+01	.2337E+02
23	.6901E+01	.4233E+02	51	.2377E+01	.2899E+02	78	.3315E+01	.2317E+02
24	.6717E+01	.4084E+02	52	.2296E+01	.2766E+02	79	.3296E+01	.2273E+02
25	.6548E+01	.3677E+02	53	.2252E+01	.2630E+02	80	.3281E+01	.2317E+02
26	.6432E+01	.3637E+02	54	.2236E+01	.2569E+02	81	.3263E+01	.2276E+02
27	.6264E+01	.3506E+02						

Table B-6. Numerical Results Generated by Using Piecewise-Constant Method With R_N From (15).

0	.1626E+02	.8910E+02	28	.6076E+01	.3726E+02	55	.2207E+01	.2738E+02
1	.1626E+02	.8910E+02	29	.5925E+01	.3756E+02	56	.2215E+01	.2676E+02
2	.1600E+02	.9114E+02	30	.5767E+01	.3840E+02	57	.2214E+01	.2659E+02
3	.1475E+02	.8799E+02	31	.5593E+01	.3701E+02	58	.2257E+01	.2694E+02
4	.1405E+02	.8026E+02	32	.5408E+01	.3632E+02	59	.2313E+01	.2532E+02
5	.1338E+02	.8319E+02	33	.5193E+01	.3460E+02	60	.2355E+01	.2588E+02
6	.1243E+02	.8064E+02	34	.4920E+01	.3364E+02	61	.2405E+01	.2739E+02
7	.1154E+02	.7202E+02	35	.4695E+01	.3246E+02	62	.2478E+01	.2752E+02
8	.1119E+02	.7375E+02	36	.4421E+01	.3046E+02	63	.2547E+01	.2667E+02
9	.1065E+02	.6653E+02	37	.4148E+01	.2824E+02	64	.2625E+01	.2653E+02
10	.1019E+02	.6623E+02	38	.3927E+01	.2746E+02	65	.2701E+01	.2685E+02
11	.9747E+01	.6054E+02	39	.3701E+01	.2471E+02	66	.2795E+01	.2610E+02
12	.9529E+01	.6435E+02	40	.3563E+01	.2504E+02	67	.2886E+01	.2582E+02
13	.9158E+01	.6301E+02	41	.3411E+01	.2419E+02	68	.2963E+01	.2663E+02
14	.8906E+01	.5755E+02	42	.3235E+01	.2460E+02	69	.3035E+01	.2649E+02
15	.8546E+01	.5747E+02	43	.3113E+01	.2472E+02	70	.3089E+01	.2546E+02
16	.8220E+01	.5388E+02	44	.2979E+01	.2492E+02	71	.3150E+01	.2512E+02
17	.7995E+01	.5349E+02	45	.2870E+01	.2516E+02	72	.3211E+01	.2433E+02
18	.7831E+01	.5034E+02	46	.2810E+01	.2512E+02	73	.3246E+01	.2417E+02
19	.7645E+01	.4933E+02	47	.2689E+01	.2579E+02	74	.3264E+01	.2382E+02
20	.7485E+01	.4904E+02	48	.2621E+01	.2563E+02	75	.3277E+01	.2303E+02
21	.7326E+01	.4877E+02	49	.2532E+01	.2615E+02	76	.3273E+01	.2296E+02
22	.7086E+01	.4474E+02	50	.2438E+01	.2662E+02	77	.3273E+01	.2257E+02
23	.6899E+01	.4238E+02	51	.2364E+01	.2790E+02	78	.3274E+01	.2301E+02
24	.6715E+01	.4081E+02	52	.2280E+01	.2728E+02	79	.3264E+01	.2292E+02
25	.6547E+01	.3669E+02	53	.2227E+01	.2697E+02	80	.3262E+01	.2322E+02
26	.6432E+01	.3640E+02	54	.2201E+01	.2680E+02	81	.3245E+01	.2292E+02
27	.6264E+01	.3503E+02						

DISTRIBUTION

Director
Strategic Systems Projects Office
Washington, DC 20376
ATTN: SP-20
SP-203
SP-231
SP-2311
SP-23115

(4)

The Charles Stark Draper Laboratory
555 Technology Square
Cambridge, MA 02139
ATTN: P. Howard
W. Robertson
M. Williamson

Lockheed Missile and Space Company
P.O. Box 504
Sunnyvale, CA 94088
ATTN: R. Crutchfield
J. Old

Lockheed Palo Alto Research Lab.
Dept. 52-56
3251 Hanover Street
Palo Alto, CA 94304
ATTN: R. Dickson

Singer-Kearfott Division
150 Totowa Road
Wayne, NJ 07470
ATTN: G. Blauth

General Electric Ordnance Systems
100 Plastics Avenue
Pittsfield, MA 01201
ATTN: D. Berube
M. Smith
J. Vreeland

(4)

U. S. Naval Oceanographic Office
NSTL Station
Bay St. Louis, MS 39522
ATTN: T. Davis

DMAAC (STT)
St. Louis Air Force Station
St. Louis, MO 63118
ATTN: B. Decker

Department of Geodetic Science
The Ohio State University
Columbus, OH 43210
ATTN: R. Rapp

NOAA–National Ocean Survey
6001 Executive Blvd.
Rockville, MD 20852
ATTN: E. Herbrechtsmeier

Aerospace Corporation
2350 East EL Segundo Blvd.
El Segundo, CA 90245
ATTN: L. Wong

Goddard Space Flight Center
Code 932
Greenbelt, MD 20771
ATTN: E. Lancaster

Department of Geophysics and Planetary Physics
The University, Newcastle-Upon-Tyne
NEI 7RU, England (UK)
ATTN: F. J. Lowes

Department of Mathematics
Old Dominion University
Norfolk, VA 23508
ATTN: J. Tweed (3)

Defense Technical Information Center (2)
Cameron Station
Alexandria, VA 22314

Local:

E41	
K01	
K10	(10)
K50	
K51	(30)
K53	
K54	
K55	(2)
X210	(2)
X211	(2)

Defense Technical Information Center (2)
Cameron Station
Alexandria, VA 22314

Local:

E41	
K01	
K10	(10)
K50	
K51	(30)
K53	
K54	
K55	(2)
X210	(2)
X211	(2)